Astrophysics, Vol. 53, No. 3, 2010

EXTRAGALACTIC H_2O MASER SOURCES AND THEIR PROPERTIES

R. A. Kandalyan[1,2] and M. M. Al-Zyout[2]

The properties of a sample of extragalactic H_2O maser sources over a wide spectral range are discussed. Based on a sample of 81 maser galaxies it is shown that mega- and kilomasers have completely different properties. In particular, for megamasers the strongest observed relationships are between the parameters of the H_2O line and the mass of the galactic nucleus, while the parameters of the line are uncorrelated with the x-ray, infrared, and radio emission. A weak correlation between megamaser emission and the surface (column) density of hydrogen is observed. As for kilomasers, their H_2O luminosity depends weakly on the x-ray emission, although in the case of soft x rays this dependence is significant. The H_2O luminosity of kilomasers is moderately correlated with the infrared and radio continuum luminosities, but the line parameters are independent of the mass of the nucleus and the surface density of hydrogen.

Keywords: maser-galaxies: active galaxies: galaxies with active star formation

1. Introduction

Extragalactic maser emission at a wavelength of 1.35 cm from the galaxy M33 was discovered in 1976 [1]. Up to now this kind of emission has been discovered from more than 105 galaxies, most of which have active nuclei [2,3]. Extragalactic maser sources are divided into two groups. Galaxies with luminosities $L_{H_2O} < 10 L_\odot$ are kilomasers and those with $L_{H_2O} \geq 10 L_\odot$ are megamasers. This division is related to the fact that kilomasers are mainly associated with galaxies that have active star formation, while megamasers, with galaxies that have active nuclei. In addition, megamasers are observed in galaxies for which the surface density (column density) of hydrogen is very high in the

(1) V. A. Ambartsumyan Byurakan Astrophysical Observatory, Armenia; e-mail: kandalyan@yahoo.com kandalyan@aabu.edu.jo
(2) Institute of Astronomy and Space Science, Al Al-Bayt University, Jordan

Original article submitted March 25, 2010; accepted for publication May 25, 2010. Translated from Astrofizika, Vol. 53, No. 3, pp. 363-376 (August 2010).

0571-7256/10/5303-0329

central region ($N_H > 10^{24}$cm^{-2}) [2,4,5]. X-ray radiation from the central part of a galaxy can heat a circumnuclear molecular cloud and stimulate water maser emission [6]. In that case, we may expect a relationship between the maser and x-ray emission. Furthermore, if megamaser emission is related to the activity of the nucleus, then a correlation between maser emission and the mass of the nucleus of a galaxy is to be expected [7,8].

Maser emission originates from a central part of a galaxy of size 1 pc or smaller. Megamasers are subdivided morphologically into three major groups: (a) disk masers, where the sources of the radiation are formed by a presumed accretion disk (e.g., NGC 4258); (b) jet masers, which lie along a stream emerging from the center of the galaxy (e.g., Mrk 348); and, (c) outflow masers, which lie along outflows from the nucleus (e.g., Circinus). This morphological classification is based primarily on *VLBI* observations [9] and as well on the spectral features of the maser emission. A slight correlation has been observed between maser and x-ray emission [7]. If the maser emission originates in an accretion disk, then there must be a correlation between the maser and x-ray emission, since accretion disks are strong x-ray sources; hence, this question is of some interest. Studies of the relationship between maser emission and the radio continuum help to clarify the mechanism for the maser emission. A correlation has been observed [10] between maser and infrared emission. Studies of the relationship between maser emission and the mass of the nucleus of a galaxy are very important. A positive correlation has been found [8] between maser emission and the mass of a black hole. A weak correlation between the luminosity of maser emission and the surface density of hydrogen has been found [4].

This paper is a more detailed study of the above mentioned features of maser emission based on a large sample of galaxies and employing the methods of nonparametric statistics. Nonparametric statistical methods provide a more correct analysis of observational data, taking possible selection effects into account, in particular the Malmqvist effect and the role of anomalous data in evaluating correlation and regression coefficients. The sample of extragalactic masers is discussed in Section 2. The nonparametric linear regression technique used in our analysis is described in Section 3. The results of the analysis are given in Section 4. Section 5 is a discussion of the results of this paper.

2. The sample of H_2O masers

As pointed out in the *introduction*, maser emission has been discovered from more than 105 galaxies. However, the parameters of the maser emission have not been reported in the literature for all these galaxies. Thus, our list of maser galaxies only includes objects for which the flux densities have been reported (March 2010) (Table 1). In those cases where there are no published widths of the emission line, we have determined it from published spectra [3]. Tables 1 lists data for 81 galaxies. This list omits only one distant galaxy J0804+3607 ($z=0.66$), which belongs to the gegamaser group and differs significantly in luminosity from the other maser galaxies over the entire spectrum. The columns of table 1 list the following in sequence: (1) Designation of the galaxy. A subscript *k* means that the given galaxy belongs to the kilomaser group. (2) Red shift, *z*. (3) Luminosity of the maser emission, L_{H_2O}, in solar units. When the luminosity value is taken from the literature, the reference is indicated. Otherwise we have calculated the luminosities. (4) The FWHM of the line in the rest system of the galaxy, *W*, in km/s. (5) The x-ray luminosity in the 0.5-2 keV range, $L_{0.5\text{-}2\text{keV}}$, in solar units. (6) The x-ray luminosity in the 2-10 keV range, $L_{2\text{-}10\text{keV}}$, in solar units. (7) The

TABLE 1. A Sample of 81 H_2O Maser Galaxies

	Galaxy(*)	Z[a]	$\log L_{H_2O}$[b]	$\log W$	$\log L_{0.5\text{-}2keV}$	$\log L_{2\text{-}10keV}$	$\log L_{60micron}$(a)	$\log L_{1.4GHz}$(a)	$\log M_c$	$\log N_H$	Refs.		
			$L_\odot$	km s^{-1}	$L_\odot$	$L_\odot$	$L_\odot$	$L_\odot$	$M_\odot$	cm^{-2}	X-ray	M_c	N_H
	1	2	3	4	5	6	7	8	9	10	11	12	13
1	NGC 23	0.02	2.20	1.57[c]			10.72	5.08					
2	IC10(SE)$_{(k)}$	0.001	-0.80	0.10	3.62	4.84		2.16		21.78	16		4
3	NGC 235A	0.02	2.00	0.94[c]	7.84			5.15			4		
4	NGC 253$_{(k)}$	0.001	-0.30	1.28	4.95	5.81	10.17	4.07	7.07	21.53	17,18	19	20
5	Mrk 348	0.02	2.61	2.12	6.93	8.9	9.65	5.69	7.99	23.20	21,7	22	4
6	ESO 013-G012	0.02	2.70[d]	1.58	5.44	7.65	10.09				e		
7	Mrk 1	0.02	1.81	0.46	5.90	8.11	10.21	5.14	7.16		e	23	
8	M33(IC133)$_{(k)}$	0.001	-0.50[d]	0.18	1.42	5.62	6.91	2.85	5.14	21.23	24,25	22	4
9	NGC 520$_{(k)}$	0.01	0.60	0.04	5.02	6.45	10.66	4.85			e		
10	NGC 591	0.02	1.40	0.30[c]	7.02	9.57	10.06	4.73	6.83	23.38	26	8	27
11	NGC 613	0.005	1.45	1.57	5.62	7.83	10.14	4.40	7.31		e	22	
12	IC 0184	0.02	1.40	1.15[c]	7.59		9.49	3.86			4		
13	NGC 1052	0.01	2.33	1.93	6.64	7.5	8.75	5.22	8.31	23.11	28,7	22	29
14	NGC 1068	0.004	2.16	0.70[c]	7.87	9.6	10.81	5.65	7.60	24	30,7	22	27
15	NGC 1106$_{(k)}$	0.01	0.86	0.00			9.82	5.29					
16	Mrk 1066	0.01	1.76	0.08	7.01	9	10.60	5.01	7.01	23.38	26,7	23	27
17	0335+0104	0.04	2.70[d]	1.54[c]			10.36	5.47					
18	NGC 1386	0.003	2.08	0.58	6.88	8.4	9.10	3.35	8.01	23.29	31,7	22	27
19	IC 342$_{(k)}$	0.0001	-1.83	-0.27	3.26	5.9	9.06	3.63	6.46	21.58	e,32	22	20
20	UGC3193	0.01	2.40	1.10[c]			10.16	4.43					
21	UGC 3255	0.02	1.20	0.92[c]	7.81		10.00	4.94			4		
22	Mrk 3	0.01	1.04	0.40[c]	7.76	9.6	10.29	6.15		23.68	33,7		27
23	NGC 2146$_{(k)}$	0.003	0.92	1.85	6.59	6.87	10.69	5.00		21.30	34,35		4
24	VII Zw 073	0.04	2.20	0.65[c]	8.50		10.87	5.14			4		
25	NGC 2273$_{(k)}$	0.01	0.83	1.53	6.36	8.1	9.78	4.22	7.30	23.64	31,7	23	27
26	UGC 3789	0.01	2.53	0.78[c]			9.71	4.16					
27	Mrk 78	0.04	1.53	0.00[c]	7.11	9.32	10.59		7.15		e	22	
28	Mrk 1210	0.01	1.99	0.43	7.38	9.3	9.94	5.16	7.15	23.33	36,7	37	4
29	He 2-10$_{(k)}$	0.003	-0.17	2.06	5.91	5.49				21.09	38		38
30	0836+3327	0.05	3.40[d]	0.85[c]									
31	NGC 2639	0.01	1.85	0.65	6.82	7	9.78	4.99	8.02	23.60	29,7	22	4
32	NGC 2782	0.01	1.08	0.08[c]	5.64	7.6	10.22	4.80	7.60	20.85	4,7	22	39
33	NGC 2824	0.01	2.70[d]	2.18	7.11		9.34	3.73	7.27		4	22	
34	0927+493	0.03	2.70[d]	1.49[c]			10.68						

TABLE 1. (Continued)

	1	2	3	4	5	6	7	8	9	10	11	12	13
35	UGC 5101	0.04	3.17	2.43	6.97	8.8	11.67	6.16		24.13	29,7		4
36	Mrk 1419	0.02	2.64	1.93[c]	5.59	8.38	9.72	4.13			e		
37	NGC 2979	0.01	2.10[d]	0.81[c]	7.08		9.47		7.12		4	37	
38	NGC 2989	0.01	1.54	1.15[c]			9.91						
39	M 82$_{(k)}$	0.001	0.24	0.79	6.75	6.81	10.50	4.59		21.08	40		4
40	NGC 3079	0.004	2.76	0.90[c]	6.28	8.4	10.28	4.96	7.63	25.00	30,7	22	30
41	IC 2560	0.01	2.12	1.39	6.34	8.3	9.79		7.56	24.48	41,42,7	37	4
42	Mrk 34	0.05	2.49	1.56	7.05	9.84	10.72		7.96		e	8	
43	NGC 3359$_{(k)}$	0.003	-0.21	0.23[c]	5.67		9.28	3.63			f		
44	NGC 3393	0.01	2.61	1.38	7.53	8.5	9.94		7.98	24.64	31,7	22	4
45	NGC 3556$_{(k)}$	0.002	0.04	1.00	4.13	5.56	9.29	4.26		21.48	43		4
46	Arp 299	0.01	2.40	2.42	6.72	8.2		5.72		24.40	29,7		4
47	NGC 3735	0.01	1.21	0.45	5.20	7.41	10.13	4.69			e		
48	NGC4038/39$_{(k)}$	0.01	0.91	0.85	6.98		10.45				f		
49	NGC 4051$_{(k)}$	0.002	0.30	0.30[c]	7.17	7.6	9.22	3.62	6.70	21.00	30,7	23	4
50	NGC 4151$_{(k)}$	0.003	-0.15	0.18	7.23	9.40	9.27	4.46	7.93	23.30	30,44	22	4
51	NGC 4214$_{(k)}$	0.001	-1.56	1.32	3.78	4.96	8.37	0.77		21.28	45		45
52	NGC 4258	0.001	1.98	0.70[c]	5.74	7	9.25	4.05	7.82	21.54	30,7	22	20
53	NGC 4293$_{(k)}$	0.003	0.62	0.65[c]	6.40		9.17	3.37			4		
54	NGC 4388	0.01	1.10	0.18[c]	6.90	8.7	10.27	4.83	7.22	23.6	30,7	22	27
55	NGC 4527$_{(k)}$	0.01	0.57	0.26[c]			10.42	4.65					
56	ESO 269-G012	0.02	3.00[d]	0.40[c]	6.18	7.04			7.75		26	37	
57	NGC 4922	0.02	2.29	1.43[c]			10.94	5.19	7.65			8	
58	NGC 4945	0.002	1.77	0.41	5.82	9.1	10.20		7.43	21.76	46,7	19	20
59	M 51$_{(k)}$	0.002	-0.10	1.11	5.99	7.7	9.81	4.47	7.13	21.36	30,7	22	20
60	NGC 5256	0.03	1.49	0.04[c]	6.99	9.3	11.15	5.94	6.92	22.34	29,7	8	29
61	NGC 5253$_{(k)}$	0.001	-1.68	0.08	2.90	4.98	8.71	2.60		22.00	38		38
62	NGC 5347	0.01	1.51	1.18	6.19	8.1	9.33	3.37	6.97	23.38	27,7	22	27
63	NGC 5495	0.02	2.30	1.15[c]	8.05		10.25				4		
64	Circinus	0.001	1.57	0.00	5.65	7.5	9.92	4.02	7.83	22.07	47,7	8	20
65	NGC 5506	0.01	1.79	-0.15	7.88	8.9	9.92	4.99	6.88	22.48	27,7	37	27
66	NGC 5643	0.004	1.40[d]	0.54[c]	6.24	7.6	9.98	4.35	6.79	23.26	48,7	37	27
67	NGC 5728	0.01	1.94	0.54[c]	6.60	8.7	10.28		8.18	23.86	27,7	22	27
68	UGC 9618B	0.03	3.20[d]	1.54[c]									
69	NGC 5793	0.01	2.29	1.15	5.29	7.31	10.35	6.01			g		
70	NGC 6240	0.02	1.98	0.66	7.74	9.8	11.53	6.25		23.7	49,7		29
71	NGC 6264	0.03	3.10[d]	1.15[c]									

TABLE 1. (Conclusion)

	1	2	3	4	5	6	7	8	9	10	11	12	13
72	NGC 6323	0.03	2.68	0.30[c]	5.28	7.49	9.69	4.17			e		
73	NGC 6300$_{(k)}$	0.004	0.50[d]	0.54[c]	5.40	8.1	9.77		6.92	23.38	50,7	37	4
74	ESO 103-G35	0.01	2.56	0.92	6.70	9.1	10.01		7.15	23.31	51,7	37	4
75	1937-0131	0.02	2.20[d]	1.48[c]	8.01		10.39				4		
76	3C403	0.06	3.30[d]	1.67[c]	7.41	9.6	10.58	8.14			52,7		
77	NGC 6926	0.02	2.70[d]	1.30[c]	7.81		10.85	5.52			4		
78	2158-380	0.03	2.70	1.36[c]	7.60		9.95	7.05			f		
79	TXS 2226-18	0.03	3.80[d]	1.88[c]	8.13	8.77	9.68				4		
80	NGC 7479	0.01	1.22	0.48[c]	5.46	7.68	10.37	4.68	7.07		e	22	
81	IC 1481	0.02	2.51	0.32	6.30	8.52	10.17	5.03			4		

Notes to Table 1: * Galaxies with subscript (k) belong to the kilomaser group; (a) Data from NASA/IPAC Extragalactic Database (NED) [53]; (b) List of known extragalactic masers and published data in Ref. 3; (c) This paper; (d) Ref. 54; (e) X-ray observations from the X-ray Multi-mirror Mission - Newton (XMM-Newton); (f) X-ray observations from the Roentgen SATellite (ROSAT); (g) X-ray observations from Chandra X-ray Observatory (CXO).

infrared luminosity at a wavelength of 60 micron, $L_{60\text{micron}}$, in solar units. (8) The radio luminosity at a frequency of 1.4 GHz, $L_{1.4\text{GHz}}$, in solar units. (9) Mass of the assumed black hole, M_c, in solar units. (10) Surface density of hydrogen, N_H, in cm^{-2}, derived from x-ray absorption. (11) References for the x-ray observations. (12) References for the mass of the black hole. (13) References for the surface density. The luminosities were calculated using the equations given in Ref. 11. The Hubble constant is taken to be $H_0 = 75$ km/s/Mpc. The notation a, b, c, d, e, and f is explained at the bottom of Table 1. If a galaxy has been observed with several x-ray telescopes, then preference is given to the Chandra telescope, then to XMM-Newton, and then to the other telescopes, since the Chandra telescope has a higher angular resolution. We have also tried to use later observational results, employing data from the HEASARC archive [12].

3. Nonparametric linear regression

Regression analysis is intended to clarify a possible relationship between two (or more) observed variables. Very often parametric linear regression is used to analyze observational data. In it, $y_i = a_0 + a_1 x_i + e_i$, where $i = 1,2,...,n$ is the number of observations; x_i is the independent variable, assumed to be determined "exactly" with no error; y_i is the dependent variable, which has a normal distribution; and, e_i is the residual error, which also has a normal distribution. It is also assumed that the observational results are independent of one another. The parametric method of linear regression has a number of disadvantages, which can significantly distort the actual relationship between the variables. Some of the major disadvantages are: (a) The distribution of y_i may not be normal (e.g., an asymmetric distribution). This is a significant shortcoming if the sample size is small ($n < 30$). However, sometimes

when $n > 30$ the sample distribution may not be normal. Thus, in each specific case it is necessary to check whether the distribution is normal or not. (b) Among the observational data there are measurements that differ greatly from the other data (so called outliers or anomalous points). Since parametric linear regression uses the means of the variables x_i and y_i and their standard deviations, including outliers in the statistic can significantly distort the actual regression line, making its slope either too steep or too flat. On the other hand, excluding outliers from the analysis reduces the sample size and, in addition, these points may not be random scatter, but actual observational results that may reflect a particular physical process. Thus, it is more appropriate to use nonparametric techniques for linear regression and correlation on samples of this sort. Here we briefly examine the Kendall-Theil nonparametric technique for linear regression which uses the method of medians.

Suppose we have the following pairs of random variables (X_i, Y_i), while the linear regression equation is $Y_i = a_0 + a_1 X_i + e_i$, i = 1,2,...,n, where X_i is the independent variable, Y_i is the dependent variable, e_i is the residual error or uncertainty in the determination of Y_i, a_0 is the intercept with the ordinate, and a_1 is the slope of the line (tangent of the angle between the regression line and the abscissa). We assume that the distributions of the variables X_i and Y_i are arbitrary. The slope of the line is given by the median value between the pairs using the formula

$$a_{ij} = \frac{Y_j - Y_i}{X_j - X_i}, \quad a_1 = \text{median}\left[a_{ij}\right],$$

where $i = 1, 2, \ldots, (n-1)$, $j = 2, 3, \ldots, n$, $i < j$, $X_j \neq X_i$. The total number of possible pairs of slopes is $n(n-1)/2$. Thus, for example, if n = 10, the total number of possible slopes to be calculated will be 45. After calculating all the possible values of the slopes, we order them in increasing sequence and find their median. This value of the median is taken to be the slope of the regression line. If the total number of paired slopes is odd, then the central term of the sequence is the median. If, on the other hand, the total number of paired slopes is even, then the median of the sequence is taken to be the average of the two central terms. The intercept is evaluated using the formula $a_0 = Y_m - a_1 X_m$, where X_m and Y_m are the medians of the independent and dependent variables, respectively. The nonparametric Kendall-Theil method has been discussed elsewhere [13].

A computer program for the Kendall-Theil method is given in Ref. 14. We have used this program, which is very convenient and useful for data analysis, in our calculations. Here we briefly list the main advantages of nonparametric linear regression: (a) the distribution does not have to be normal. (b) It can be used for small samples. (c) Outliers in the sample do not affect the results of the calculations, since the average values of the variables and their standard deviations do not appear in the calculations.

4. Analysis of results

According to the Kolmogorov-Smirnov statistic, almost all the parameters listed in Table 1 have non-normal distributions. Hence, the use of nonparametric regression and correlation techniques is justified in the case of our sample of masers. First of all, we calculated the Spearman rank-order correlation coefficients [15] between the

TABLE 2. Statistical Parameters of the Three Samples

Parameter	Megamasers			Kilomasers			All masers		
	N	Avg.	Stand. error	*N*	Avg.	Stand. error	*N*	Avg.	Stand. error
z	60	0.018	0.002	21	0.0034	0.0007	81	0.014	0.001
$\log W$	60	0.98	0.08	21	0.67	0.14	81	0.90	0.07
$\log L_{\mathrm{H_2O}}$	60	2.18	0.08	21	-0.04	0.18	81	1.60	0.13
$\log L_{0.5\text{-}2}$	50	6.79	0.13	19	5.24	0.38	69	6.36	0.16
$\log L_{2\text{-}10}$	40	8.44	0.13	16	6.51	0.34	56	7.89	0.18
$\log L_{60}$	54	10.15	0.08	19	9.54	0.21	73	9.99	0.08
$\log L_{1.4}$	42	5.04	0.14	18	3.80	0.27	60	4.67	0.15
$\log M_c$	31	7.46	0.08	8	6.83	0.29	39	7.33	0.09
$\log N_H$	26	23.28	0.19	15	21.80	0.23	41	22.75	0.19

parameters listed in Table 1, including the red shift. In those cases where the variables in some pair also depend on the red shift (the so-called Malmqvist effect), we used the partial Spearman coefficients in order to eliminate the Malmqvist effect from the given correlation. After this analysis we selected those pairs of variables which exhibit significant correlation coefficients after the Malmqvist effect had been taken into account. (By significance in the correlation we mean that the probability of a random correlation between the variables $P \le 0.05$.) We did this analysis separately for the megamasers and kilomasers, as well as for all of the masers together.

Table 2 lists the basic statistical data (number of galaxies N, its mean and standard error) for all the parameters listed in Table 1.

Table 3 lists the results of the statistical analysis, where the most significant partial Spearman correlations ρ, with the Malmqvist effect taken into account, are indicated. The pairs of variables for which the Spearman correlation coefficients are of low significance, are not listed in Table 3. Also shown there are the results of a Kendall-Theil linear regression (slope *S*, intercept *I*, 95% confidence interval for the slope, and median deviation *d*). If the median deviation *d* is close to zero, then the linear regression is the appropriate approximation. In Table 3, $\log L_{\mathrm{H_2O}}$ and $\log W$ are the dependent variables, while the other variables are independent. In particular, the regression line between $\log L_{\mathrm{H_2O}}$ and $\log M_c$ for the megamasers has the form $\log L_{\mathrm{H_2O}} = 0.6 \log M_c - 2.52$.

We found no substantial correlations between the parameters of the H_2O emission line ($L_{\mathrm{H_2O}}$ and *W*) and the luminosities $L_{0.5\text{-}2\mathrm{keV}}$, $L_{2\text{-}10\mathrm{keV}}$, $L_{60\mathrm{micron}}$, and $L_{1.4\mathrm{GHz}}$ for the megamasers. Thus, for example, $\rho(L_{\mathrm{H_2O}}, L_{2\text{-}10\mathrm{keV}})$ = 0.02 (with N = 40, P=0.91).

As for the kilomasers, the most significant correlations and the corresponding regression parameters are given in Table 3. Also shown there are the data for the entire set of masers.

Table 3 shows that the emission from the mega- and kilomasers have entirely different dependences on the

TABLE 3. Correlation and Regression Coefficients for the Three Samples

Megamasers				
	$\log M_c$	$\log N_H$	$\log M_c$	$\log N_H$
$\log L_{H_2O}$	N = 31 ρ = 0.52 P = 0.002	N = 26 ρ = 0.39 P = 0.05	S = 0.60 I = -2.52 $0.17 \le S \le 0.98$ D = -0.14	S = 0.28 I = -4.47 $-0.006 \le S \le 0.48$ d = 0.007
$\log W$	N = 31 ρ = 0.41 P = 0.02	N = 26 ρ = 0.47 P = 0.01	S = 0.55 I = -3.47 $0.03 \le S \le 1.14$ D = 0.03	S = 0.32 I = -6.94 $0.06 \le S \le 0.61$ d = -0.02
Kilomasers				
	$\log L_{(0.5\text{-}2)\text{keV}}$	$\log L_{(2\text{-}10)\text{keV}}$	$\log L_{60\text{micron}}$	$\log L_{1.4\text{GHz}}$
$\log L_{H_2O}$	N = 19 ρ = 0.59 P = 0.01 S = 0.34 I = -2.05 $0.14 \le S \le 0.61$ d = 0.005	N = 16 ρ = 0.48 P = 0.08 S = 0.40 I = -2.59 $0.09 \le S \le 0.80$ d = -0.14	N = 19 ρ = 0.56 P = 0.02 S = 0.59 I = -5.49 $0.17 \le S \le 1.31$ d = -0.05	N = 18 ρ = 0.53 P = 0.03 S = 0.55 I = -2.30 $0.37 \le S \le 0.95$ d = 0.24
All masers				
	$\log M_c$	$\log N_H$	$\log M_c$	$\log N_H$
$\log L_{H_2O}$	N = 39 ρ = 0.59 $P = 7 \cdot 10^{-5}$	N = 41 ρ = 0.35 P = 0.02	S = 0.94 I = -5.07 $0.55 \le S \le 1.42$ d = -0.13	S = 0.63 I = -13.13 $0.37 \le S \le 0.88$ d = 0.15
$\log W$	N = 39 ñ = 0.42 $P = 8 \cdot 10^{-3}$	No correlation	S = 0.44 I = - 2.69 $0.11 \le S \le 0.94$ d = 0.01	

other parameters of the galaxies. Once again, this emphasizes the fact that these maser sources are associated with different processes taking place in the galaxies. As the set of all masers, their behavior essentially repeats that of the megamasers, except for the relationship between $\log W$ and $\log N_H$.

5. Discussion

As noted above, in megamaser galaxies the maser and x-ray radiation are formed in the circum-nuclear region. Thus, given the activity of the nucleus, we might expect that the maser emission to depend on the mass of the galactic nucleus. The mass of the nucleus can be estimated assuming that an accretion disk and black hole lie at the center of the galaxy. Unfortunately, other assumptions about the nucleus of a galaxy do not make it possible to estimate the mass of the nucleus. Figure 1 is a plot of $\log L_{H_2O}$ as a function of $\log M_c$ for the megamasers, together with the Kendall-Theil regression line.

The x-ray emission from the accretion disk in megamasers can stimulate [6] collisional pumping of the H_2O maser emission level by heating a molecular cloud. In that case we should expect a positive correlation between the maser and x-ray emission. In terms of this theory, the hard x-ray emission should be proportional to the mass of the nucleus [7], while the maser emission increases as the square of the mass of the nucleus [8]. Up to now, however, no reliable correlation between the maser and x-ray emission has been found in megamasers (cf. Ref. 6 and Table 3). According to our analysis, there is also no correlation between the x-ray emission and the mass of the nucleus. A relationship between L_{H_2O} and M_c does exist (Table 3, $L_{H_2O} \sim M_c^{0.6}$), but it is not quadratic, as the theory [6,8] implies. In Ref. 8 it was noted that $L_{H_2O} \sim M_c^{3.6}$, but our data do not confirm such a dependence. In addition, based on the observations reported in Ref. 8, our analysis revealed no such relationship between L_{H_2O} and M_c. According to Ref. 8, $M_c \sim L_{H_2O}^{0.28}$, and it seems to us that these authors used this dependence to find that $L_{H_2O} \sim M_c^{1/0.28} = M_c^{3.6}$. If this is so, then this procedure is not correct, since the relationship between L_{H_2O} and M_c is statistical and the inverse relationship cannot be determined in this way. The results of Table 3 show that for the megamasers the strongest relationships are observed between the parameters of the H_2O line and the mass of the galactic nucleus.

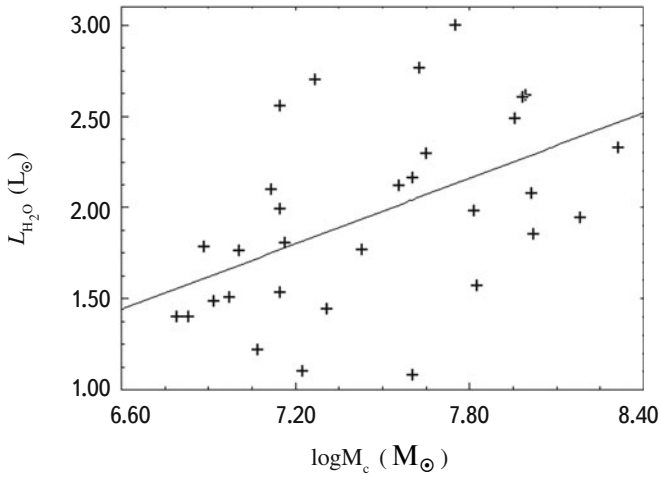

Fig. 1. Relation between megamaser emission and the mass of the galactic nucleus. The regression line is also shown (see Table 3).

The shape of the H_2O line is the a result of the distribution and kinematics of the gas. Line broadening is caused either by dispersion of the velocities among individual clouds or by rotation of the central part of the galaxy. The simultaneous occurrence of both can also lead to broadening of the line. If we regard the line width W as a measure of the rotation of the disk about the galactic nucleus, then the linear rotation velocity is $V = (GM_c/R)^{0.5}$, where G is the gravitational constant and R is the disk radius. Table 3 shows that $W \sim M_c^{0.55}$, and this relationship is close to that expected between V and M_c. Figure 2 is a plot of $\log W$ as a function of $\log M_c$ for the megamasers, together with the Kendall-Theil linear regression.

The dependences of $\log L_{H_2O}$ and W on N_H are significant, but weak. The luminosity of the maser radiation increases exponentially with the surface density of molecules if the radiation is not saturated. If, on the other hand, the radiation is saturated, then $L_{H_2O} \sim N_H^2$ in the presence of a velocity gradient.

According to Table 3, an entirely different picture is observed in the case of the kilomasers. The isotropic H_2O luminosity depends weakly on the x-ray emission, although this dependence is significant in the case of soft x rays. At the same time, the L_{H_2O} luminosity has a moderate correlation with the luminosities in the far infrared and radio continuum. The parameters of the radio line do not depend on the mass of the nucleus (although it should be noted that in this case the number of galaxies with known M_c is small, at $N = 8$, for reliable statistics) and the surface density of hydrogen. This behavior of the maser radiation is difficult to explain uniquely, although if we adhere to the view that the main factor determining the properties of the galaxy in kilomasers is star formation activity, rather than activity of the nucleus, then a dependence of L_{H_2O} on these luminosities is to be expected.

We also analyzed galaxies belonging to the morphological group of disk-shaped megamasers (N = 52). The properties of this sample differ little from those of the sample of megamasers. Thus, as an example, for the disk-shaped megamasers $\log L_{H_2O} = 0.56 \log M_c - 2.17$ with a correlation coefficient of $\rho = 0.48$, $P = 0.01$, and $N = 25$.

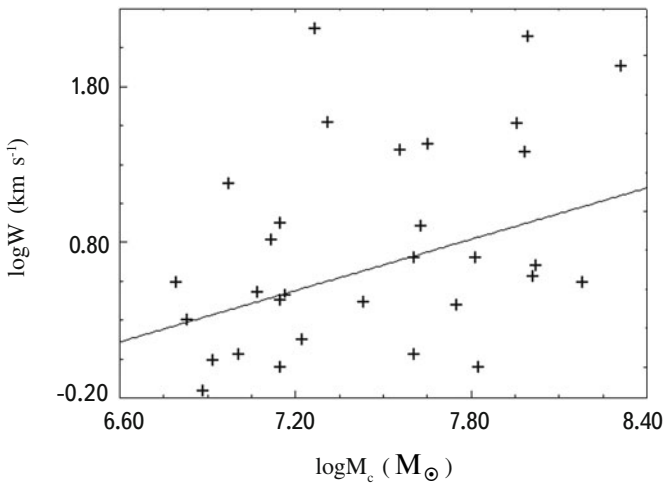

Fig. 2. Relation between the width of the megamaser emission line and the mass of the galactic nucleus. The regression line is also shown (see Table 3).

The fact that the intensity of the maser radiation and the line width in megamasers depend on the mass of the nucleus means that the molecular cloud is being acted on by an active nucleus. Our results are inconsistent with the theoretical proposition that megamaser and x-ray emission are related, but this question may require further study. It seems to us that the results of this paper cannot be explained in terms of the existing theories on the relationship between maser radiation and the activity of galactic nuclei.

6. Conclusion

We have studied a sample of extragalactic H_2O maser sources over a wide spectral range. In our analysis we have used a nonparametric linear regression and correlation technique. The basic results of our work are the following: (1) Mega- and kilomasers have entirely different properties. In particular, in megamasers the strongest interrelations are observed between the parameters of the H_2O line and the mass of the galactic nucleus ($L_{H_2O} \sim M_c^{0.6}$, $W \sim M_c^{0.55}$), while the parameters of the line are uncorrelated with the x-ray, infrared, and radio emissions. A weak correlation is observed between the megamaser emission and the surface density of hydrogen. (2) In the kilomasers the H_2O luminosity depends weakly on the x-ray emission, although this dependence is significant in the case of soft x rays. The H_2O luminosity of kilomasers correlates moderately with the luminosities in the infrared and radio continuum, but the parameters of the line are independent of the mass of the nucleus and the surface density of hydrogen. (3) The fact that the luminosity of the maser emission and the line width in megamasers depend on the mass of the nucleus implies that in these galaxies the maser cloud is acted on by the galactic nucleus and an active nucleus determines the major properties of the galaxy. In kilomasers the major factor determining the properties of the galaxy is star formation activity, rather than the activity of the nucleus.

REFERENCES

1. E. Churchwell, A. Witzel, W. Huchtmeier, et al., *Astron. Astrophys* **54**, 969 (1977).
2. J. S. Zhang, C. Henkel, Q. Gue, et al., *Astrophys. J.* **708**, 1528 (2010).
3. J. A. Braatz, http://wiki.gb.nrao.edu/bin/view/Main/WaterMaserList (2009).
4. J. S. Zhang, C. Henkel, M. Kadler, et al., *Astron. Astrophys.* **450**, 933 (2006).
5. L. J. Greenhill, A. Tilak, and G. Madejski, *Astrophys. J.* **686**, L13 (2008).
6. D. A. Neufeld, P. R. Maloney, and S. Conger, *Astrophys. J.* **436**, L127 (1994).
7. P. T. Kondratko, L. J. Greenhill, and J. M. Moran, *Astrophys. J.* **652**, 136 (2006).
8. J. B. Su, J. S. Zhang, and J. H. Fan, Chin. J. *Astron. Astrophys.* **8**, 547 (2008).
9. L. J. Greenhill, P. T. Kondratko, J. M. Moran, and A. Tilak, *Astrophys. J.* **707**, 787 (2009).
10. C. Henkel, A. B. Peck, A. Tarchi, et al., *Astron. Astrophys.* **436**, 75 (2005).
11. R. A. Kandalyan, *Astron. Astrophys.* **404**, 513 (2003).
12. HEASARC, http://heasarc.gsfc.nasa.gov/db-perl/W3Browse/w3browse.pl (2010).

13. W. L. Conover, Practical Non-parametric Statistics, 2nd Ed. New York, John Wiley and Sons (1980).
14. G. E. Granato, http://pubs.usgs.gov/tm/2006/tm4a7/TM4A7/ktrlinedownloads.htm (2010).
15. R. A. Kandalyan, *Astrophysics* **39**, 417 (1996).
16. F. E. Bauer and W. N. Brandt, **Astrophys. J. 601**, L67 (2004).
17. R. Barnard, L. Shaw Greening, and U. Kolb, *Mon. Notic. Roy. Astron. Soc.* **388**, 849 (2008).
18. K. A. Weaver, T. M. Heckman, D. K. Strickland, and M. Dahlem, *Astrophys. J.* **576**, L19 (2002).
19. E. Oliva, L. Origlia, R. Mailino, and A. F. M. Moorwood, *Astron. Astrophys.* **350**, 9 (1999).
20. L. M. Winter, R. F. Mushotzky, and C. S. Reynlods, *Astrophys. J.* **649**, 730 (2006).
21. H. Awaki, S. Ueno, Y. Taniguchi, and K. Weaver, *Astrophys. J.* **542**, 175 (2000).
22. D. B. McElroy, *Astrophys. J. Suppl. Ser.* **100**, 105 (1995).
23. C. H. Nelson and M. Whittle, *Astrophys. J. Suppl. Ser.* **99**, 67 (1995).
24. R. Tullmann, K. S. Long, T. G. Pannuti, et al., *Astrophys. J.* **707**, 1361 (2009).
25. L. Foschini, J. Rodrigues, Y. Fuchs, et al., *Astron. Astrophys.* **416**, 529 (2004).
26. M. Guainazzi, G. Matt, and G. C. Perola, *Astron. Astrophys.* **444**, 119 (2005).
27. C. N. Cardamone, E. C. Moran, and L. E. Kay, *Astron. J.* **134**, 1263 (2007).
28. L. W. Brenneman, K. A. Weaver, M. Kadler, et al., *Astrophys. J.* **698**, 528 (2009).
29. O. Gonzalez-Martin, J. Masegosa, I. Marquez, M. Guainazzi, and E. Jimenez-Bailon, *Astron. Astrophys.* **506**, 1107 (2009).
30. M. Cappi, F. Panessa, L. Bassani, et al., *Astron. Astrophys.* **446**, 459 (2006).
31. M. Guainazzi, A. C. Fabian, K. Iwasawa, G. Matt, and F. Fiore, *Mon. Notic. Roy. Astron. Soc.* **356**, 295 (2005).
32. A. K. H. Kong, *Mon. Notic. Roy. Astron. Soc.* **346**, 265 (2003).
33. S. Bianchi, G. Miniutti, A. C. Fabian, and K. Iwasawa, *Mon. Notic. Roy. Astron. Soc.* **360**, 380 (2005).
34. T. Inui, H. Matsumoto, T. G. Tsuru, et al., *Publ. Astron. Soc. Japan,* **57**, 135 (2005.
35. R. Della Ceca, R. E. Griffiths, T. M. Heckman, M. D. Lehnert, and K. A. Weaver, *Astrophys. J.* **514**, 772 (1999).
36. M. Guainazzi, G. Matt, F. Fiore, and G. C. Perola, *Astron. Astrophys.* **388**, 787 (2002).
37. R. Cid Fernandes, Q. Gu, J. Melnick, et al., *Mon. Notic. Roy. Astron. Soc.* **355**, 273 (2004).
38. J. Ott, F. Walter, and E. Brinks, *Mon. Notic. Roy. Astron. Soc.* **358**, 1453 (2005).
39. P. Tzanavaris and I. Georgantopoulos, *Astron. Astrophys.* **468**, 129 (2007).
40. P. Kaaret, M. G. Simet, and C. C. Lang, *Astrophys. J.* **646**, 174 (2006).
41. K. Iwasawa, P. R. Maloney, and A. C. Fabian, *Mon. Notic. Roy. Astron. Soc.* **336**, L71 (2002).
42. G. Madejski, C. Done, P. T. Zychi, and L. Greenhill, *Astrophys. J.* **636**, 75 (2006).
43. Q. D. Wang, T. Chaves, and J. A. Irwin, *Astrophys. J.* **598**, 969 (2003).
44. K. A. Weaver, J. Gelbord, and T. Yaqoob, *Astrophys. J.* **550**, 261 (2001).
45. J. M. Hartwell, I. R. Stevens, D. K. Strickland, T. M. Heckman, and L. K. Summers, *Mon. Notic. Roy. Astron. Soc*. **348**, 406 (2004).
46. M. Guainazzi, G. Matt, W. N. Brandt, et al., *Astron. Astrophys.* **356**, 463 (2000).
47. M. Guainazzi, G. Matt, L. A. Antonelli, et al., *Mon. Notic. Roy. Astron. Soc.* **310**, 10 (1999).
48. M. Guainazzi, P. Rodriguez-Pascual, A. C. Fabian, K. Iwasawa, and G. Matt, *Mon. Notic. Roy. Astron. Soc.* **355**, 297 (2004).
49. A. Ptak, T. Heckman, N. A. Levenson, K. Weaver, and D. Strickland, *Astrophys. J.* **592**, 782 (2003).

50. C. Matsumoto, A. Nava, L. A. Maddox, et al., *Astrophys. J.* **617**, 930 (2004).

51. K. Noguchi, Y. Terashima, and H. Awaki, *Astrophys. J.* **705**, 454 (2009).

52. R. P. Kraft, M. J. Hardcastle, D. M. Worral, and S. S. Murray, *Astrophys. J.* **622**, 149 (2005).

53. NASA/IPAC Extragalactic Database, http://nedwww.ipac.caltech.edu/ (2010).

54. N. Bennert, R. Barvainis, C. Henkel, and R. Antonucci, *Astrophys. J.* **695**, 276 (2009).